Inorganic Materials, Vol. 41, No. 10, 2005, pp. 1089–1096. From Neorganicheskie Materialy, Vol. 41, No. 10, 2005, pp. 1236–1242.
Original English Text Copyright © 2005 by Hiroaki Onoda, Daisuke Mori, Kazuo Kojima, Hiroyuki Nariai.

Mechanochemical Effects on the Formation and Properties of Various Nickel Phosphates*

Hiroaki Onoda[1,2], Daisuke Mori[2], Kazuo Kojima[2], and Hiroyuki Nariai[3]

[1] *Department of Materials Science and Engineering, Faculty of Engineering, Kyoto University,*
Yoshida-Honmachi, Sakyo-ku, Kyoto 606-8501, Japan

[2] *Department of Applied Chemistry, Faculty of Science and Engineering, Ritsumeikan University, 1-1-1,*
Nojihigashi, Kusatsu, Shiga 525-8577, Japan

[3] *Department of Molecular Science and Materials Engineering, Graduate School of Science and Technology,*
Kobe University, 1-1, Rokkodai-cho, Nada-ku, Kobe 657-8501, Japan

e-mail: onoda@se.ritsumei.ac.jp

Received February 24, 2005; in final form April 19, 2005

Abstract—Mixtures of ammonium dihydrogen phosphate and basic nickel carbonate with P/Ni molar ratios of 2/3, 1/1, and 2/1 were ground in a planetary mill. The thermal behavior of the milled samples was investigated by differential thermal analysis, x-ray diffraction, and Fourier transform infrared spectroscopy. In addition, the samples were characterized by ultraviolet–visible reflectance spectroscopy, particle size distribution, scanning electron microscopy, and nitrogen adsorption measurements. As a result of mechanochemical effects, the targeted nickel phosphates were formed at lower temperatures, had a more vivid color, and consisted of more regularly shaped particles.

INTRODUCTION

Phosphates transform to other phosphates in hydrolysis and dehydration reactions at elevated temperatures [1, 2]. The group of condensed phosphates includes polyphosphates, cyclophosphates, and ultraphosphates. Polyphosphates have a chain structure in which each PO_4 unit shares two oxygen atoms with other PO_4 units. Cyclophosphates have a cyclic structure, and ultraphosphates have a network structure [3].

Phosphates are used for the preparation of ceramics, catalysts, fluorescent materials, dielectrics, metal surface treatment agents, detergents, food additives, fuel cell materials, pigments, etc. In general, inorganic phosphate pigments are prepared by mixing starting materials, followed by calcination, crushing, and adjusting their color. There are reports on the calcination temperature and time, but less information about the mixing of starting materials. Because the particle shape and size distribution influence many properties, for example, the color of pigments, the study of the mixing of starting materials is important for the development of new inorganic functional materials.

The physical and chemical properties of solids are influenced by crushing, pressing, milling, and other mechanical treatments [4–8]. These phenomena are known as mechanochemical effects and lead to an increase in specific surface area, defect density, and strain; bond cleavage; and other processes. Owing to these effects, mechanically treated materials are regarded as being in an active state. Such mechanical treatments have been applied to inorganic materials. Using mechanical treatment, new materials, higher yields, and lower temperature sintering can be achieved.

In previous work, mechanochemical effects were investigated in mixtures of ammonium dihydrogen phosphate, manganese carbonate, and neodymium oxide in the molar ratios P/(2Mn + 3Nd) = 1/2 and Mn/Nd = 10/0, 9/1, and 8/2 [9]. In these systems, since the mixed materials were mechanically activated, $Mn_2P_2O_7$ was formed at lower temperature. During mechanical treatment, the change of hue was observed at a lower temperature, and phosphates had a more vivid color. Mechanochemical treatment of starting materials was shown to be effective method of producing functional inorganic materials.

In this work, we assess the mechanochemical effect on the formation and properties of various nickel phosphates from ammonium dihydrogen phosphate and basic nickel carbonate.

EXPERIMENTAL

Mixtures of ammonium dihydrogen phosphate, $NH_4H_2PO_4$, and basic nickel carbonate, $NiCO_3 \cdot 2Ni(OH)_2 \cdot 4H_2O$, with P/Ni molar ratios of 2/3, 1/1, and 2/1 were ground in a Fritsch planetary mill for several minutes. These ratios are the same as those in nickel orthophosphate, $Ni_3(PO_4)_2$, nickel pyrophos-

---

* The text was submitted by the authors in English.

phate, $Ni_2P_2O_7$, and nickel cyclotetraphosphate, $Ni_2P_4O_{12}$. The mill had five ZrO_2 balls (15-mm diameter) and a ZrO_2 vessel (40-mm inner diameter, 40-mm height). The thermal behavior of the mixtures was studied by differential thermal analysis (DTA), x-ray diffraction (XRD), and Fourier transform infrared (FTIR) spectroscopy. DTA was carried out with a Rigaku Denki DTA50 at a heating rate of 10°C/min. XRD patterns were recorded on a Rigaku Denki RINT 2000M diffractometer using monochromatized CuK_α radiation. IR spectra were recorded on a Shimadzu FT-IR8600 spectrometer using a KBr disk method.

The thermal products heat-treated at different temperatures for 1 h were characterized by ultraviolet–visible (UV–Vis) reflectance spectroscopy, scanning electron microscopy (SEM), particle size distribution, and specific surface area measurements. UV–Vis reflectance spectra were measured with a Shimadzu UV-3101PC. SEM images were obtained using a Hitachi F-4300. Particle size distributions were measured with a laser diffraction/scattering particle size distribution HORIBA LA-910. The specific surface area of phosphates was evaluated from the amount of nitrogen gas adsorbed at liquid-nitrogen temperature by the BET method using a Belsorp mini (BEL JAPAN).

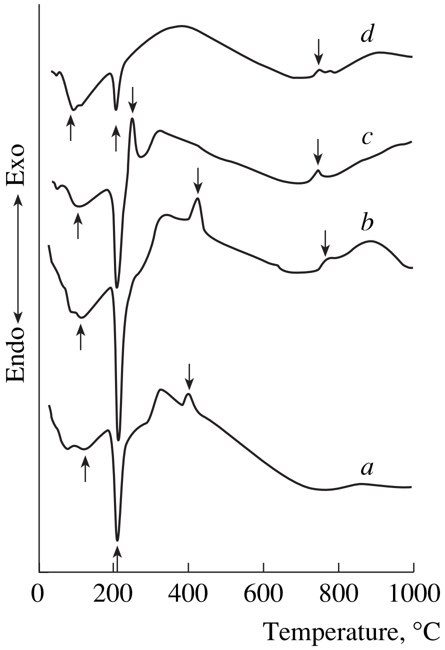

Fig. 1. DTA curves of samples with P/Ni = 2/3: (*a*) without milling; (*b*–*d*) milling for 10, 20, and 30 min, respectively.

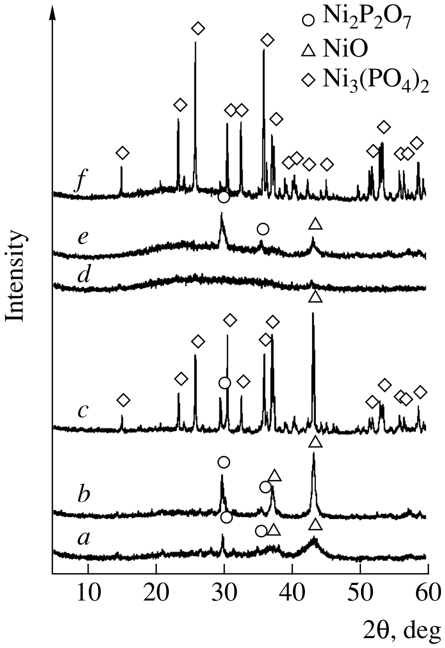

Fig. 2. XRD patterns of samples with P/Ni = 2/3: (*a*–*c*) without milling, (*d*–*f*) milling for 30 min; heat treatment at (*a*, *d*) 500, (*b*, *e*) 700, and (*c*, *f*) 1000°C.

RESULTS AND DISCUSSION

Formation of Nickel Orthophosphate

Figure 1 shows DTA curves of samples with P/Ni = 2/3 milled for several minutes. All of the DTA curves have endothermic peaks below 150 and at 200°C. The endothermic peak at 200°C becomes weaker with increasing milling time. The unmilled sample has an exothermic peak at 400°C (Fig. 1, curve *a*). The sample milled for 10 min has exothermic peaks at 425 and 770°C (Fig. 1, curve *b*). The sample milled for 20 min has exothermic peaks at 250 and 745°C (Fig. 1, curve *c*). The exothermic peak at 750°C is also present in the DTA curve of the sample milled for 30 min (Fig. 1, curve *d*).

Figure 2 shows the XRD patterns of the samples without milling and milled for 30 min and then heated at different temperatures. The peaks of $Ni_2P_2O_7$ and NiO were observed in the XRD patterns of the unmilled samples heated at 500 and 700°C (Fig. 2, scans *a*, *b*). The XRD pattern of the sample heated at 1000°C has the peaks of NiO, $Ni_3(PO_4)_2$, and $Ni_2P_2O_7$ (Fig. 2, scan *c*). The sample milled for 30 min and heated at 500°C is x-ray amorphous (Fig. 2, scan *d*). The peaks of $Ni_2P_2O_7$ and NiO were observed in XRD pattern of the sample heated at 700°C (Fig. 2, scan *e*). The XRD pattern of the sample heated at 1000°C is similar to that of $Ni_3(PO_4)_2$ (Fig. 2, scan *f*). Figure 3 shows the IR spectra of the samples with P/Ni = 2/3 heated at 700°C. The samples without milling and milled for 10 min had absorption peaks due to $Ni_2P_4O_{12}$ and $Ni_2P_2O_7$ (Fig. 3, spectra *a*, *b*) [10]. The peaks of $Ni_2P_4O_{12}$ in the IR spectrum of the sample milled for 10 min were stronger than those of the unmilled sample. The samples milled for 20 and 30 min had the adsorption peaks due to $Ni_2P_2O_7$ (Fig. 3, spectra *a*, *b*).

The XRD and FT-IR data for the P/Ni = 2/3 samples are summarized in Table 1. Nickel oxide was formed in the unmilled sample by the reaction

$$NiCO_3 \cdot 2Ni(OH)_2 \cdot H_2O \longrightarrow 3NiO + CO_2 + 6H_2O. \quad (1)$$

The endothermic peaks below 150 and at 200°C in the DTA curves of milled and unmilled samples are due to the volatilization of water and ammonia, respectively (Fig. 1). Mechanical treatment caused the volatilization of water and ammonia. The sample milled for 30 min had weaker endothermic peaks. The exothermic peaks at 400 and 450°C in the DTA curves of the samples without milling and milled for 10 min are probably related to the formation of $Ni_2P_4O_{12}$ (Fig. 1, curves *a*, *b*; Table 1). The intensities of these exothermic peaks corresponded to those of the IR absorption peaks of $Ni_2P_4O_{12}$. However, $Ni_2P_4O_{12}$ was generally formed in an endothermic dehydration reaction. It was difficult to clarify the origin of these peaks in this work. It was also difficult to explain the higher $Ni_2P_4O_{12}$ content of the sample milled for 10 min compared to the unmilled sample (Fig. 3). $Ni_2P_4O_{12}$ was considered to be formed according to the schemes [11]

$$\begin{gathered} NiCO_3 \cdot 2Ni(OH)_2 \cdot 4H_2O + 6NH_4H_2PO_4 \\ \longrightarrow 3Ni(H_2PO_4)_2 + CO_2 + 6NH_3 + 9H_2O, \end{gathered} \quad (2)$$

$$2Ni(H_2PO_4)_2 \longrightarrow Ni_2P_4O_{12} + 4H_2O. \quad (3)$$

At higher temperatures, the following chemical reactions were also considered in the samples without milling and milled for 10 min:

$$Ni_2P_4O_{12} + 2NiO \cdot 2Ni_2P_2O_7, \quad (4)$$

$$Ni_2P_4O_{12} + 4NiO \cdot 2Ni_3(PO_4)_2. \quad (5)$$

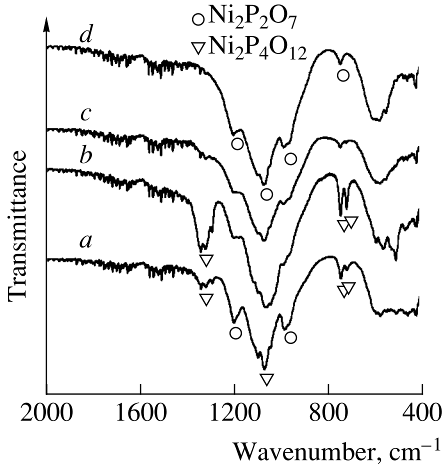

Fig. 3. IR spectra of samples with P/Ni = 2/3 heat-treated at 700°C: (*a*) without milling; (*b*–*d*) milling for 10, 20, and 30 min, respectively.

The exothermic peak at 250°C in the DTA curve of the sample milled for 20 min was considered to be due to the formation of $NiHPO_4$ (Fig. 1, curve *c*) [9]. $Ni_2P_2O_7$ was formed through $NiHPO_4$ by the reactions

$$\begin{gathered} NiCO_3 \cdot 2Ni(OH)_2 \cdot 4H_2O + 3NH_4H_2PO_4 \\ \longrightarrow 3NiHPO_4 + CO_2 + 3NH_3 + 9H_2O, \end{gathered} \quad (6)$$

$$2NiHPO_4 \longrightarrow Ni_2P_2O_7 + H_2O. \quad (7)$$

These reactions were considered to occur in other samples. However, the exothermic peak at 250°C was not observed in DTA curves (Fig. 1, curves *a*, *b*, *d*). It was difficult to rationalize these results in this work. The following chemical reaction was also considered in the sample milled for 20 min at higher temperatures:

$$Ni_2P_2O_7 + NiO \longrightarrow Ni_3(PO_4)_2. \quad (8)$$

The small exothermic peaks at about 750°C were considered to be due to $Ni_3(PO_4)_2$ crystallization.

Table 1. Thermal products with P/Ni = 2/3 obtained at different temperatures

Milling time, min	Thermal products				
	250°C	350°C	500°C	700°C	1000°C
0	Amorphous	NiO	$NiO + Ni_2P_2O_7$	$NiO + Ni_2P_2O_7 + Ni_2P_4O_{12}$	$NiO + Ni_3(PO_4)_2 + Ni_2P_2O_7$
10	Amorphous	Amorphous	Amorphous	$NiO + Ni_2P_2O_7 + Ni_2P_4O_{12}$	$Ni_3(PO_4)_2 + Ni_2P_2O_7$
20	Amorphous	Amorphous	Amorphous	$Ni_2P_2O_7 + NiO$	$Ni_3(PO_4)_2$
30	Amorphous	Amorphous	Amorphous	$Ni_2P_2O_7 + NiO$	$Ni_3(PO_4)_2$

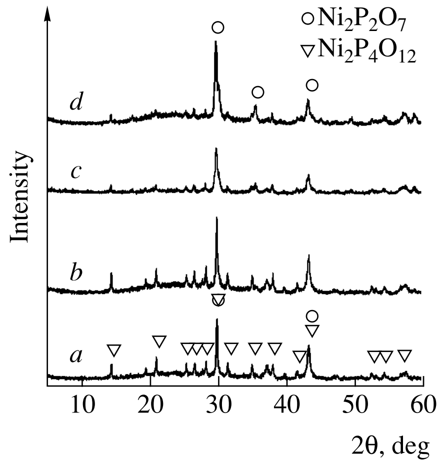

Fig. 4. XRD patterns of samples with P/Ni = 1/1 heat-treated at 700°C: (*a*) without milling; (*b*–*d*) milling for 10, 20, and 30 min, respectively.

$Ni_3(PO_4)_2$ was finally formed in the P/Ni = 2/3 system by the overall reaction

$$NiCO_3 \cdot 2Ni(OH)_2 \cdot 4H_2O + 2NH_4H_2PO_4 \longrightarrow Ni_3(PO_4)_2 + CO_2 + 2NH_3 + 9H_2O. \quad (9)$$

Sufficient mechanical treatment prevented nickel oxide formation. It was considered that nickel orthophosphate was formed not by way of NiO.

Formation of Nickel Pyrophosphate

Thermal products in the P/Ni = 1/1 system were less changed by mechanical treatment than those with P/Ni = 2/3. Figure 4 shows the XRD patterns of samples milled for several minutes and heated at 700°C. The peaks of $Ni_2P_4O_{12}$ and $Ni_2P_2O_7$ were observed in the XRD patterns of the samples without milling and milled for 10 min (Fig. 4, scans *a*, *b*). The peaks of $Ni_2P_4O_{12}$ became weaker upon mechanical treatment (Fig. 4, scans *c*, *d*).

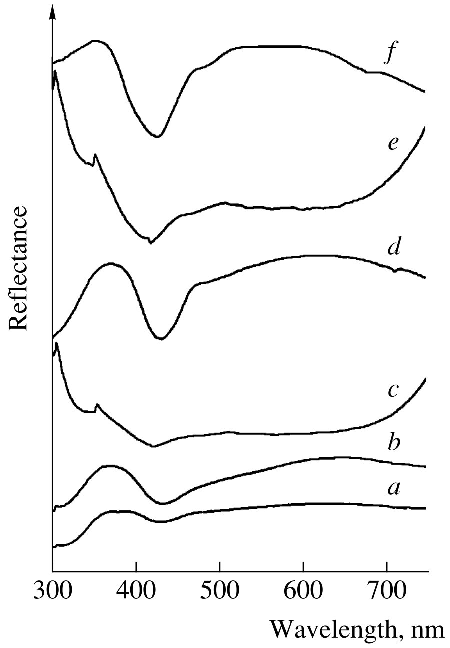

Fig. 5. UV–Vis reflectance spectra of thermal products obtained at 700°C: P/Ni = (*a*, *b*) 2/3, (*c*, *d*) 1/1, (*e*, *f*) 2/1; (*a*, *c*, *e*) without milling, (*b*, *d*, *f*) milling for 30 min.

The XRD and FT-IR data for the P/Ni = 1/1 samples are summarized in Table 2. As a result of the mechanochemical effect, $Ni_2P_2O_7$ became easier to prepare at 700 and 1000°C. It was considered that $Ni_2P_4O_{12}$ was formed by Eqs. (2) and (3) and then reacted with NiO to form $Ni_2P_2O_7$ by Eq. (4).

Formation of Nickel Cyclotetraphosphate

Since $NH_4H_2PO_4$ is highly reactive, $Ni_2P_4O_{12}$ is easy to prepare in the P/Ni = 2/1 system. Therefore, the changes of thermal products were less pronounced in this system. The XRD and FT-IR data for the P/Ni = 2/1 samples are summarized in Table 3. The samples without milling and milled for 10 min and then heated at 1000°C consisted of $Ni_2P_4O_{12}$ and $Ni_2P_2O_7$, while the samples milled for 20 and 30 min consisted of $Ni_2P_4O_{12}$

Table 2. Thermal products with P/Ni = 1/1 obtained at different temperatures

Milling time, min	Thermal products			
	300°C	500°C	700°C	1000°C
0	Amorphous	$Ni_2P_4O_{12}$	$Ni_2P_4O_{12}$ + $Ni_2P_2O_7$	$Ni_2P_2O_7$ + $Ni_2P_4O_{12}$
10	Amorphous	$Ni_2P_4O_{12}$	$Ni_2P_4O_{12}$ + $Ni_2P_2O_7$	$Ni_2P_2O_7$
20	Amorphous	$Ni_2P_4O_{12}$	$Ni_2P_2O_7$	$Ni_2P_2O_7$
30	Amorphous	$Ni_2P_4O_{12}$	$Ni_2P_2O_7$	$Ni_2P_2O_7$

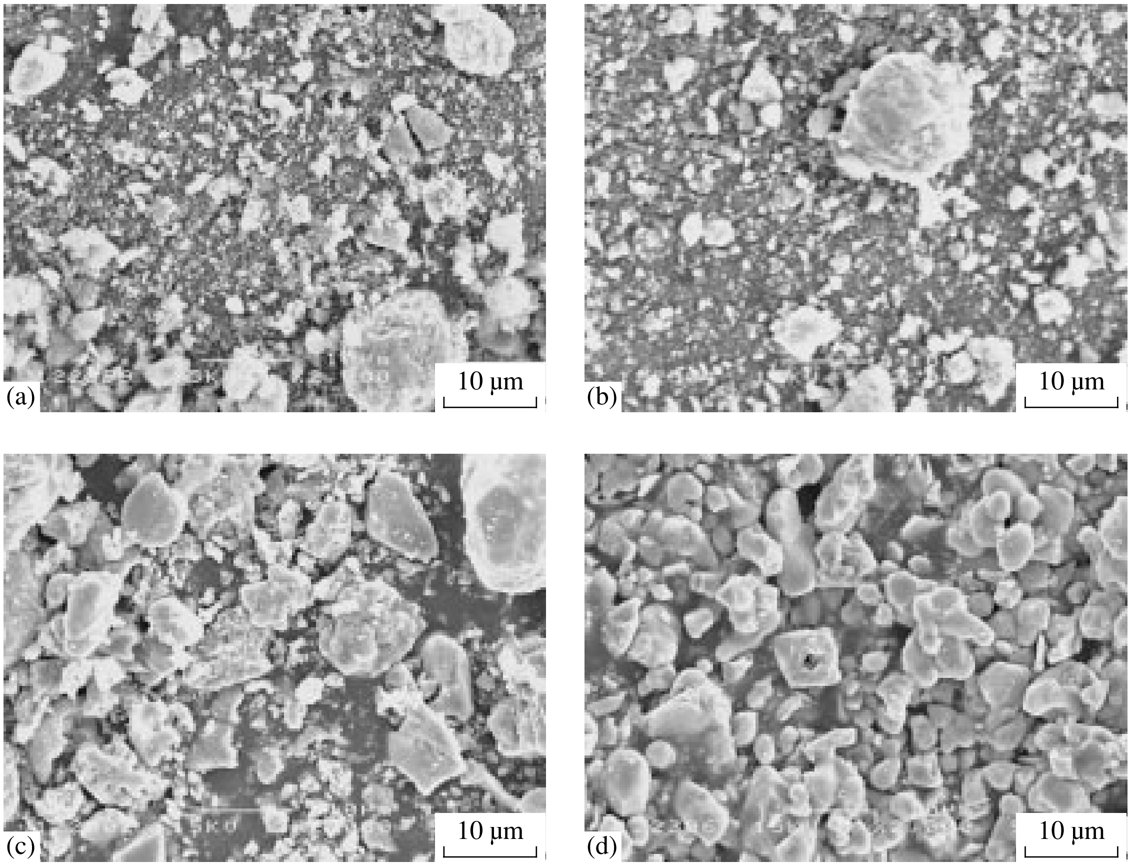

Fig. 6. SEM images of thermal products with P/Ni = 2/3: (a) without milling, 700°C; (b) milling for 30 min, 700°C; (c) without milling, 1000°C; (d) milling for 30 min, 1000°C.

only. Nickel cyclotetraphosphate was formed by Eqs. (2) and (3) and transformed to nickel pyrophosphate at high temperatures with P_2O_5 volatilization:

$$Ni_2P_4O_{12} \longrightarrow Ni_2P_2O_7 + P_2O_5. \quad (10)$$

Hue of Thermal Products

Figure 5 shows the UV–Vis reflectance spectra of the thermal products at 700°C. The samples with P/Ni = 2/3 had low reflectance (Fig. 5, spectra *a*, *b*). The P/Ni = 2/3 samples without milling and milled for 30 min were dark and light gray, respectively. After mechanical treatment, the thermal products with P/Ni = 2/3 had a vivid color. It was thought to be related to NiO formation. Mechanochemical effects were clearly observed in the UV–Vis reflectance spectra of the thermal products with P/Ni = 1/1 and 2/1 (Fig. 5, spectra *c*–*f*). The samples without milling had low reflectance, while the samples milled for 30 min had high reflectance. The P/Ni = 1/1 samples without milling and milled for 30 min were gray and light

Table 3. Thermal products with P/Ni = 2/1 obtained at different temperatures

Milling time, min	Thermal products			
	300°C	500°C	700°C	1000°C
0	Amorphous	$Ni_2P_4O_{12}$	$Ni_2P_4O_{12}$	$Ni_2P_4O_{12} + Ni_2P_2O_7$
10	Amorphous	$Ni_2P_4O_{12}$	$Ni_2P_4O_{12}$	$Ni_2P_4O_{12} + Ni_2P_2O_7$
20	Amorphous	$Ni_2P_4O_{12}$	$Ni_2P_4O_{12}$	$Ni_2P_4O_{12}$
30	Amorphous	$Ni_2P_4O_{12}$	$Ni_2P_4O_{12}$	$Ni_2P_4O_{12}$

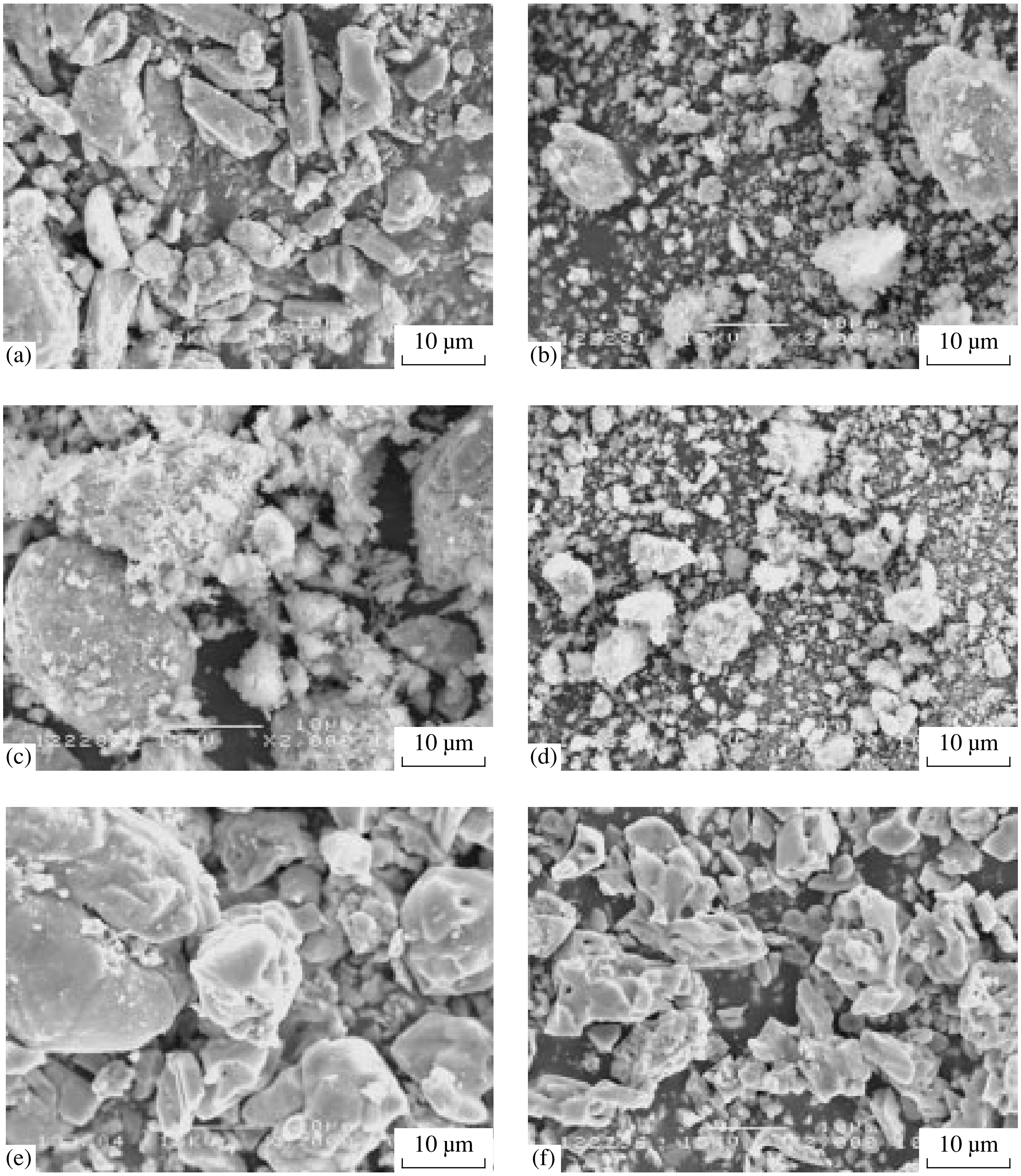

Fig. 7. SEM images of thermal products with P/Ni = 1/1: (a–c) without milling, (d–f) milling for 30 min; heat treatment at (a, b) 500, (c, d) 700, and (e, f) 1000°C.

green, respectively. The P/Ni = 2/1 thermal products without milling and milled for 30 min were light green and lighter green, respectively. After mechanical treatment, the thermal products with P/Ni = 1/1 and 2/1 also had a vivid color tone at the same temperature. At lower temperatures, the samples were dark owing to the presence of nickel oxide. The samples had a brighter color at higher heat-treatment temperatures. Mechanical treatment produced inorganic phosphate pigments at lower temperatures. Condensed nickel phosphates had a clearer color compared to nickel orthophosphate.

Powder Properties of Thermal Products

The particle shape and size distribution are of interest from many viewpoints. The study of the particle shape and size distribution is important in the development of new inorganic functional materials.

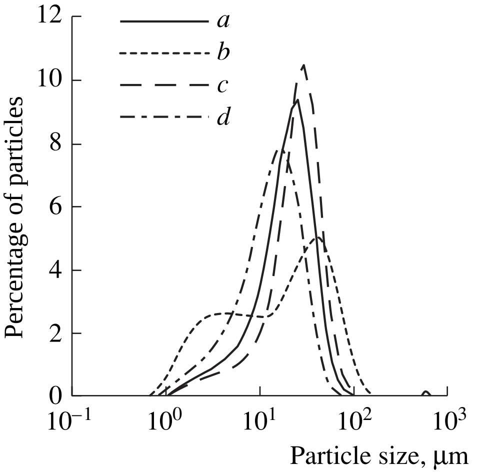

Fig. 8. Particle size distributions of thermal products: (*a*) without milling, 500°C; (*b*) milling for 30 min, 500°C, (*c*) without milling, 1000°C; (*d*) milling for 30 min, 1000°C.

Figure 6 shows SEM images of thermal products with P/Ni = 2/3 at 700 and 1000°C. The particle shape of the thermal products obtained below 700°C was insensitive to mechanical treatment (Figs. 6a, 6b), in contrast to that of the thermal products obtained at 1000°C (Figs. 6c, 6d). The sample milled for 30 min and heated at 1000°C had some degree of regularity in the particle shape. Figure 7 shows SEM images of the thermal products with P/Ni = 1/1 obtained at different temperatures. The unmilled sample heated at 500°C consisted of large particles (Fig. 7a). On the other hand, many small particles were observed in the samples milled for 30 min and heated at 500 and 700°C (Figs. 7b, 7d). Many large rounded particles were observed in the unmilled samples heated at 700 and 1000°C (Figs. 7c, 7e). The sample milled for 30 min and heated at 1000°C had some degree of regularity in the particle shape (Fig. 7f). The samples with P/Ni = 2/1 also had more regularity in the particle shape after mechanical treatment.

Figure 8 shows the particle size distribution of thermal products with P/Ni = 1/1. The samples heated at lower temperatures had much broad distributions after mechanical treatment (Fig. 8, curves *a*, *b*). The particle size distribution of the sample milled for 30 min and heated at 500°C consisted of two normal distributions. After mechanical treatment, the particle size was smaller, and then larger particles were formed by heating. This sample consisted of particles in two size ranges. In the samples heated at the higher temperature, smaller particles were obtained as a result of the mechanochemical effect (Fig. 8, curves *c*, *d*). The thermal products with P/Ni = 2/3 and 2/1 also had a smaller particle size after mechanical treatment. The particle size distribution of the samples depended slightly on the degree of dehydration/condensation of the phosphate, but it was difficult to find the regularity.

Table 4. Specific surface area of thermal products obtained at 700°C

P/Ni	Specific surface area, m^2/g	
	without milling	milled for 30 min
2/3	12.8	10.2
1/1	8.1	7.4
2/1	2.3	1.0

Table 4 shows the specific surface area data for the thermal products obtained at 700°C. In all of the systems, mechanical treatment reduced the specific surface area. Since the particle size decreased as a result of the mechanochemical effect (Fig. 8), it was considered that nickel phosphate particles had higher density. The specific surface area of the thermal products decreased as the degree of dehydration/condensation of the phosphates and the heat-treatment temperature increased.

CONCLUSIONS

The formation of nickel ortho-, pyro-, and cyclotetraphosphates from ammonium dihydrogen phosphate and basic nickel carbonate was studied. Owing to mechanical treatment, the targeted nickel phosphates were obtained at lower temperatures. The thermal products had a vivid color and regular particle shape as a result of mechanochemical effects. The particle size distribution and specific surface area of the thermal products were also influenced by mechanical treatment.

REFERENCES

1. Averbuch-Pouchat, M.T. and Durif, A., *Topics in Phosphate Chemistry,* Singapore: World Scientific, 1996.
2. Onoda, H., Nariai, H., Moriwaki, A., *et al.*, Formation and Catalytic Characterization of Various Rare Earth Phosphates, *J. Mater. Chem.*, 2002, vol. 12, no. 6, pp. 1754–1760.
3. Hong, H.Y-P., Crystal Structure of Neodymium Metaphosphate and Ultraphosphate, *Acta Crystallogr., Sect. B: Struct. Crystallogr. Cryst. Chem.*, 1974, vol. 30, pp. 468–474.
4. Kim, W., Zhang, Q., and Saito, F., Mechanochemical Synthesis of Hydroxyapatite from $Ca(OH)_2$–P_2O_5 and CaO–$Ca(OH)_2$–P_2O_5 Mixtures, *J. Mater. Sci.*, 2000, vol. 35, pp. 5401–5404.
5. Yeong, K.C.B., Wang, J., and Ng, S.C., Mechanochemical Synthesis of Nanocrystalline Hydroxyapatite from CaO and $CaHPO_4$, *Biomaterials*, 2001, vol. 22, pp. 2705–2712.

6. Kudaka, K., Iizuka, K., Sasaki, T., and Izumi, H., Effect of Milling Media on the Reaction Kinetics of the Mechanochemical Synthesis of Pentatitanium Trisilicate, *J. Am. Ceram. Soc.*, 2000, vol. 83, pp. 2887–2889.
7. Onoda, H., Nariai, H., Maki, H., and Motooka, I., Mechanochemical Effects on Synthesis of Rhabdophane-Type Neodymium and Cerium Phosphates, *Mater. Chem. Phys.*, 2002, vol. 78, no. 2, pp. 400–404.
8. Onoda, H., Nariari, H., Maki, H., and Motooka, I., Mechanochemical Effects of Some Rare-Earth Ultraphosphates and Reforming of Their Surface for Catalytic Properties, *Phosphorus Res. Bull.*, 1999, vol. 9, pp. 69–74.
9. Onoda, H., Sugino, N., Kojima, K., and Nariai, H., Mechanochemical Effects on Synthesis and Properties of Manganese–Neodymium Diphosphates, *Mater. Chem. Phys.*, 2003, vol. 82, no. 3, pp. 831–836.
10. Corbridge, D.E.C. and Lowe, E.J., The Infra-Red Spectra of Some Inorganic Phosphorus Compounds, *J. Chem. Soc.*, 1954, vol. 493, pp. 4555–4564.
11. Trojan, M., A Study of the Reactions during Formation of *c*-$Ni_2P_4O_{12}$, *Thermochim. Acta*, 1990, vol. 160, no. 2, pp. 361–366.